Robust Prescribed Performance Control and Adaptive Learning for the Longitudinal Dynamics of Fixed-Wing UAVs

S. Tzeranis, P. S. Trakas, X. Papageorgiou, K. J. Kyriakopoulos and C. P. Bechlioulis

***Abstract*— The objective of this work is to simultaneously control and identify the nonlinear longitudinal dynamics of small-scale fixed-wing Unmanned Aerial Vehicles (UAVs). The main difficulty in this endeavor lies in the satisfaction of the Persistence of Excitation (PE) condition, which eventually ensures accurate learning. Towards this direction, our key components comprise Radial Basis Function - Neural Networks (RBF-NNs), which are suitable mathematical models for universal function approximation, alongside with: i) the recently developed Dynamic Regression Extension and Mixing (DREM) technique; a new procedure for designing parameter estimators with enhanced performance, as well as ii) a novel control design for the longitudinal UAV dynamics utilizing the Prescribed Performance Control (PPC) methodology, which enables robust trajectory tracking with predetermined transient and steady state quality, even in the presence of model uncertainties.**

***Index Terms*— Prescribed Performance Control, System Identification, Dynamic Regression, Extension and Mixing.**

I. Introduction

The operation of UAVs as well as of most physical systems, is modeled by nonlinear differential equations. Knowledge of their form and the underlying nonlinearities facilitates the solution of a variety of significant problems, including model-based control; prediction of the system's behavior; real-time fault detection, and others. However, typically, system dynamics is partially or even completely unknown; which justifies the development of methodologies leading to their adaptive identification. Despite the significant results that have been achieved so far on adaptive control, the problem of successful learning and control of unknown system dynamics in a certain predefined domain of operation remains still open in nonlinear system identification. Moreover, adaptive control does not perform satisfactorily under strongly coupled, nonlinear systems, such as UAVs. Additionally, a quickly adaptable control scheme is needed for the multitude of commercial and custom-made UAVs that fly every day, each with slightly different model parameters.

The advent of Artificial Neural Networks (ANNs) and particularly of RBF-NNs has provided a powerful tool in the field of adaptive nonlinear system identification. Owing to their universal approximation capabilities [1], RBF-NNs have been widely used to deal with unknown nonlinearities in many applications. Nevertheless, the goal of accurate learning via RBF-NNs is difficult to be achieved unless a PE condition is met. The concept of PE has appeared widely in the adaptive identification literature and it is well known that standard parameter estimation algorithms applied to linear regression give rise to a linear time-varying system, which is exponentially stable if and only if a PE condition is imposed on the regressor vector; a fundamental result that constitutes one of the main building blocks of identification in adaptive control theories [2], [3]. Regarding RBF-NNs, the investigation of the PE property has attracted continuing efforts [4]–[7], and while different approaches were studied, the main idea is that the satisfaction of the PE property requires the network inputs to periodically pass nearby the RBF centers [5].

The adaptive identification scheme presented in this paper, is based on the recently developed DREM technique [8], which has been already implemented in various identification and adaptive control problems [9]–[12]. DREM estimators achieve better transient performance than classical gradient based or least-squares estimators in the sense that, independently of excitation conditions, the procedure guarantees monotonous response for each element contained in the vector of parameter error, which is stronger than just guaranteeing the norm's monotonicity of the corresponding vector. In addition, convergence is established with a milder PE condition for the regressor vector, namely a non-square integrability condition on the determinant of a designer-dependent regressor matrix. On the other hand, to establish the PE condition, the PPC methodology [13] will be employed for the UAV longitudinal motion control. The proposed state feedback controller isolates the output performance from the control gains selection and exhibits strong robustness against model uncertainties, while completely avoiding the explosion of complexity issue. Based on the PPC methodology, we shall develop a novel control scheme for the UAV longitudinal motion, capable of tracking airspeed and altitude trajectory profiles with predetermined quality, even in the presence of model uncertainties. Concluding, the main contributions of this work are summarized as follows:

- We design a novel robust control scheme to track airspeed and altitude trajectory profiles that guarantees the PE condition for the adopted regressors, thus, achieving actual learning of the UAV longitudinal dynamics in a predefined domain of operation.
- Compared to other parameter estimation algorithms, we ensure enhanced performance during the identification of the UAV longitudinal dynamics by employing the recently developed DREM technique.

S.T. and K.J.K. are with the Control Systems Lab, School of Mechanical Engineering, National Technical University of Athens, Greece. P.S.T., X.P. and C.P.B. are with the Department of Electrical and Computer Engineering, University of Patras, Greece. Email: chmpechl@upatras.gr.

Manuscript 14 submitted to 2022 10th International Conference on Systems and Control. Received August 13, 2022.

II. Problem Formulation and Preliminaries

A fixed-wing UAV is modeled as a 6-DoF rigid body. However, in this work, we focus only on the longitudinal dynamics. In such model, the forces and moments that act on the UAV body are primarily owing to three sources, i.e., gravity, aerodynamics and propulsion. Thus, assuming a flat Earth model, which is rather reasonable for small scale UAVs [14], the equations of motion are given as:

$$\dot{h} = V \sin\gamma \tag{1}$$

$$\dot{V} = \frac{T(V,\Phi)\cos\alpha - D(\alpha,V)}{m} - g\sin\gamma \tag{2}$$

$$\dot{\gamma} = \frac{T(V,\Phi)\sin\alpha + L(\alpha,V)}{mV} - \frac{g}{V}\cos\gamma \tag{3}$$

$$\dot{\theta} = q \tag{4}$$

$$\dot{q} = \frac{M(\alpha,V,q,\delta_\epsilon)}{Jyy} \tag{5}$$

where V is the airspeed vehicle velocity, h is the altitude, θ and γ denote the pitch and flight-path angle respectively, α = θ - γ is the angle-of-attack and q is the pitch rate. The control input signals comprise the throttle Φ and the elevator $\delta\epsilon$. Furthermore, the lift, drag and thrust forces as well as the pitch moment are denoted by $L(\alpha,V)$, $D(\alpha,V)$, $T(V,\Phi)$ and $M(\alpha,V,q,\delta_\epsilon)$, respectively, with their explicit analytic forms described in [14]. Finally, $T(V,\Phi)$ and $M(\alpha,V,q,\delta_\epsilon)$ are linear, strictly increasing and decreasing functions of Φ and δ_ϵ, respectively.

The main objective of this study is to design a robust controller, capable of tracking appropriately the selected airspeed and altitude trajectory profiles such that the UAV dynamics (1)-(5) is sufficiently excited to enable its identification.

A. Prescribed Performance Control

Prescribed performance control [13] aims at achieving convergence of a scalar tracking error $e(t)$ to a predetermined arbitrarily small residual set with speed of convergence no less than a prespecified value, which is formulated rigorously by $e(t)$ evolving strictly within a predefined region that is upper and lower bounded by certain functions of time, as follows:

$$-\rho(t) < e(t) < \rho(t),\ \forall t \geq 0, \tag{6}$$

where $\rho(t)$ denotes a smooth and bounded function of time that satisfies $\lim_{t\to\infty}\rho(t) > 0$, called performance function. For instance, an exponentially decaying performance function is given by $\rho(t) = (\rho_0 - \rho_\infty)e^{-\lambda t} + \rho_\infty$, where ρ_0, ρ_∞, λ are positive parameters. In particular, the constant ρ_0 is selected such that $\rho_0 > |e(0)|$. Moreover, the parameter $\rho_\infty \triangleq \lim_{t\to\infty}\rho(t) > 0$, which represents the maximum allowable value of the steady state error, can be set to a value reflecting the resolution of the measurement device, so that the error $e(t)$ practically converges to zero. Finally, the constant λ determines the decreasing rate of $\rho(t)$ and thus is used to set a lower bound on the convergence rate of $e(t)$. Therefore, the appropriate selection of the performance function $\rho(t)$ imposes certain transient and steady state performance characteristics on the tracking error $e(t)$.

The key point in prescribed performance control is a transformation of the tracking error $e(t)$ that modulates it with respect to the corresponding transient and steady state performance specifications, encapsulated in the performance function $\rho(t)$. More specifically, we employ a strictly increasing, odd and bijective mapping $T_f : (-1,1) \to (-\infty,\infty)$. In this work, we adopt the mapping $\epsilon(t) \triangleq T_f(\xi(t)) = \frac{1}{2}\ln\left(\frac{1+\xi(t)}{1-\xi(t)}\right)$ that meets the aforementioned properties, with $\xi(t) \triangleq \frac{e(t)}{\rho(t)}$ denoting the modulated error. Furthermore, the Jacobian (derivative) of the map $T_f(\cdot)$, which is strictly positive by construction, is defined as $T_f'(\xi) = \frac{1}{1-\xi^2}$. Owing to the properties of the aforementioned transformation, it can be easily verified [15] that preserving the boundedness of $\epsilon(t)$ is sufficient to achieve prescribed performance in the sense of (6).

B. RBF Neural Networks and Persistence of Excitation

Radial Basis Function-Neural Networks will be employed in this study owing to their universal approximation capabilities [1]. Mathematically, they are formulated as:

$$y(x) = \sum_{i=1}^{q} z_i^T(x)w_i = Z^T(x)W \tag{7}$$

where $x \in \mathbb{R}^n$ and $y \in \mathbb{R}$ denote the input and output of the RBF-NN, respectively, $W = [w_1 \cdots w_q]^T$ is the q-dimensional vector of the synaptic weights and $Z(x) = [z_1(x) \cdots z_q(x)]^T$ is a q-dimensional vector of regressor terms. In this work, we employ Gaussian functions of the form $z_i(x) = \exp\left(-\frac{(c_i - x)^2}{\sigma_i^2}\right)$, where $c_i \in \mathbb{R}^n$ and σ_i denote the center and variance of the respective kernel. Both parameters will be fixed in our analysis, thus resulting in a linearly parameterized model with respect to the synaptic weights.

The physical interpretation of the PE condition is that the regressor vector sequence spans the full dimension of the input parameter space. For RBF-NNs specifically, it was shown in [5] that the regressor vector $Z(x(t)) = \begin{bmatrix} z_1(x(t)) & \cdots & z_q(x(t)) \end{bmatrix}$ of the RBFs $z_i(\cdot)$ with centers $c_i, i = 1,\ldots,q$ is persistently exciting if the orbit $x : [0,\infty) \to \mathbb{R}^n$ is periodic and within each period it visits disjoint neighborhoods of each center c_i of the RBF-NN for a minimum amount of time.

C. Dynamic Regression Extension and Mixing Technique

Consider a linear regression problem of the form:

$$y(t) = m^T(t)\theta \tag{8}$$

where $y \in \mathbb{R}$ and $m \in \mathbb{R}^q$ are known, bounded functions of time and $\theta \in \mathbb{R}^q$ is a q-dimensional vector of unknown, though constant, parameters. The first step in DREM is to introduce $q-1$ linear, L_∞-stable operators $H_i : L_\infty \to L_\infty, i \in 1,2,\ldots,q-1$. It is stated in [8] that such operators can be either simple LTI filters or pure delay operators. In our work, we chose LTI filters of the form $H_i(s) = \frac{a_i}{s+b_i}$, with $a_i \neq 0$ and $b_i > 0$. The next step is to apply those filters

Manuscript 14 submitted to 2022 10th International Conference on Systems and Control. Received August 13, 2022.

to the original regression form (8) to generate the filtered regressions:

$$y_{f_i}(t) = m_{f_i}^T(t)\theta\,, i = 1 \cdots q-1. \tag{9}$$

Subsequently, augmenting the original regression (8) with the filtered ones (9), we obtain the extended system:

$$Y_e(t) = M_e^T(t)\theta \tag{10}$$

with $Y_e \in \mathbb{R}^q$ defined as $Y_e = [y\ y_{f_1} \dots\ y_{f_{q-1}}]^T$ and $M_e \in \mathbb{R}^{qxq}$ a square matrix defined as $M_e = [m\ m_{f_1} \dots\ m_{f_{q-1}}]$. Finally, premultiplying (10) with the adjugate matrix of M_e, we obtain a decoupled regression problem:

$$Y(t) \triangleq [Y_1(t), \dots, Y_q(t)]^T \triangleq \mathrm{adj}(M_e(t))Y_e(t) = \phi(t)\theta \tag{11}$$

with $\phi(t) = \det(M_e(t))$, from which the unknown parameters θ_i, $i = 1, \dots, q$ can be estimated separately by the adaptive laws:

$$\dot{\hat{\theta}}_i = \gamma_i\phi(Y_i - \phi\hat{\theta}_i),\ \gamma_i > 0. \tag{12}$$

Remark 1: Substituting (11) in (12) and invoking the solution of the first order differential equation of the parametric error dynamics, we conclude:

$$\lim_{t\to\infty} \tilde{\theta}_i(t) = 0 \iff \phi(t) \notin L_2^{[0,\infty)}, \tag{13}$$

where $\tilde{\theta}_i = \hat{\theta}_i - \theta_i$ denotes the parametric error. The aforementioned equivalence implies that convergence is established without invoking the usually restrictive PE condition. However, if $\phi(t)$ is PE then $\hat{\theta}_i$ converges to θ_i exponentially fast [9].

III. Control Design and Adaptive Learning

A. Control Scheme

Consider the fixed-wing UAV longitudinal dynamics (1)-(5). Since the fundamental maneuvers for the longitudinal motion are acceleration/deceleration and climb/descend, the desired motion will be dictated by the airspeed $V_d(t)$ and altitude $h_d(t)$ reference profiles, while the desired flight-path angle $\gamma_d(t)$ will be extracted by the kinematics (1). More specifically,

Step 1. Given some smooth and bounded desired altitude $h_d(t)$ and airspeed $V_d(t)$ trajectories, we consider an altitude feedback loop:

$$\dot{h}_d(t) - k_h(h - h_d) = V_d(t)\sin(\gamma_d(t)) \tag{14}$$

with $k_h > 0$, from which the desired flight-path angle trajectory is calculated as:

$$\gamma_d(t) = \arcsin\left(\frac{\dot{h}_d(t) - k_h(h - h_d)}{V_d(t)}\right) \tag{15}$$

Notice that (14) is equivalent to (1) as the altitude tracking error $h - h_d$ tends to zero, which is described in Remark 2.

Step 2. Select exponential performance functions $\rho_V(t) = (\rho_0^V - \rho_\infty^V)e^{-\lambda^V t} + \rho_\infty^V$ and $\rho_\gamma(t) = (\rho_0^\gamma - \rho_\infty^\gamma)e^{-\lambda^\gamma t} + \rho_\infty^\gamma$ that satisfy $\rho_0^V > |V(0) - V_d(0)|$ and $\rho_0^\gamma > |\gamma(0) - \gamma_d(0)|$ incorporating, via the appropriate selection of ρ_∞^V, ρ_∞^γ, λ^V and λ^γ, the desired performance specifications regarding the steady state error and the speed of convergence, as described in Subsection II-A. Subsequently, define the transformed errors:

$$\epsilon_V = T_f\left(\frac{V - V_d(t)}{\rho_V(t)}\right),\quad \epsilon_\gamma = T_f\left(\frac{\gamma - \gamma_d(t)}{\rho_\gamma(t)}\right) \tag{16}$$

Step 3. Select the reference force vector

$$\begin{bmatrix} F_x \\ F_z \end{bmatrix} \triangleq -\begin{bmatrix} k_V r_V \epsilon_V \\ \frac{k_\gamma}{V} r_\gamma \epsilon_\gamma \end{bmatrix},\ k_V, k_\gamma > 0 \tag{17}$$

with the scaling factors $r_V \triangleq \frac{T_f'\left(\frac{V - V_d(t)}{\rho_V(t)}\right)}{\rho_V(t)}$, $r_\gamma \triangleq \frac{T_f'\left(\frac{\gamma - \gamma_d(t)}{\rho_\gamma(t)}\right)}{\rho_\gamma(t)}$. Notice that the control signal F_x regulates the horizontal motion of the vehicle while F_z corresponds to the command associated with the vertical motion of the plant. Thus, utilizing the polar coordinates, we design the throttle command Φ and the reference angle of attack α_d as $\begin{bmatrix} \Phi \\ \alpha_d \end{bmatrix} = \begin{bmatrix} \sqrt{F_x^2 + F_z^2} \\ \arctan(\frac{F_z}{F_x}) \end{bmatrix}$.

Step 4. Consider the pitch reference command:

$$\theta_d(t) = \alpha_d(t) + \gamma_d(t) \tag{18}$$

and select an exponential performance function $\rho_\theta(t) = (\rho_0^\theta - \rho_\infty^\theta)e^{-\lambda^\theta t} + \rho_\infty^\theta$ to satisfy $\rho_0^\theta > |\theta(0) - \theta_d(0)|$ and incorporate the desired performance specifications via the appropriate selection of ρ_∞^θ and λ^θ. Then, the pitch rate reference control signal is designed as:

$$q_d(\theta, t) = -k_\theta T_f\left(\frac{\theta - \theta_d(t)}{\rho_\theta(t)}\right),\ k_\theta > 0 \tag{19}$$

Step 5. Finally, select an exponential performance function $\rho_q(t) = (\rho_0^q - \rho_\infty^q)e^{-\lambda^q t} + \rho_\infty^q$ that only satisfies $\rho_0^q > |q(0) - q_d(\theta(0), 0)|$ and design the elevator control command as:

$$\delta_\epsilon(\theta, q, t) = k_q T_f\left(\frac{q - q_d(\theta, t)}{\rho_q(t)}\right),\ k_q > 0 \tag{20}$$

Remark 2: Concerning the altitude kinematics (14), given the fact that we enforce prescribed performance on the airspeed and flight-path angle response, the altitude error $h - h_d$ response will be dictated by a stable, linear system with an exponentially decaying input that corresponds to the performance functions $\rho_V(t)$ and $\rho_\gamma(t)$. Thus, k_h, as well as the performance specifications encapsulated by the airspeed and flight-path angle performance functions, will define the transient and steady state response of the altitude error. Finally, notice that the elevator control signal obtains a positive sign as it is associated with the primary control deflection of the elevator. By convention [14], since $M(\alpha, V, q, \delta_\epsilon)$ is strictly decreasing, a positive elevator deflection results in a nose-down pitching moment and vice-versa.

B. Stability Analysis

Consider the positive definite and radially unbounded Lyapunov candidate function:

$$\mathcal{L} = \frac{1}{2}m(k_V\epsilon_V^2 + k_\gamma\epsilon_\gamma^2)$$

Differentiating with respect to time, substituting (2)-(3) and invoking basic trigonometric identities, we obtain:

$$\begin{aligned}\dot{\mathcal{L}} =& \frac{k_V \epsilon_V r_V}{\rho_V}\Big(T\cos\alpha_d(\cos e_\alpha - \sin e_\alpha) - D - \\ & - m\left(g\sin\gamma - \dot{V}_d - \dot{\rho}_V \xi_V\right)\Big) \\ & + \frac{k_\gamma \epsilon_\gamma r_\gamma}{\rho_\gamma V}\Big(T\sin\alpha_d(\sin e_\alpha + \cos e_\alpha) + LV \\ & - m\left(\frac{g\cos\gamma}{V} - \dot{\gamma}_d - \dot{\rho}_\gamma \xi_\gamma\right)\Big)\end{aligned} \tag{21}$$

Finally, adding and subtracting the reference force vector (17) and after straightforward algebraic manipulations, we arrive that:

$$\begin{aligned}\dot{\mathcal{L}} \leq & -\bar{k}\left\|\begin{bmatrix}\epsilon_V \\ \epsilon_\gamma\end{bmatrix}^T \begin{bmatrix} r_V & 0 \\ 0 & r_\gamma\end{bmatrix}\begin{bmatrix}1 & 0 \\ 0 & \frac{1}{V}\end{bmatrix}\begin{bmatrix}\frac{1}{\rho_V} & 0 \\ 0 & \frac{1}{\rho_\gamma}\end{bmatrix}\right\|^2 \\ & + \left\|\begin{bmatrix}\epsilon_V \\ \epsilon_\gamma\end{bmatrix}^T \begin{bmatrix} r_V & 0 \\ 0 & r_\gamma\end{bmatrix}\begin{bmatrix}1 & 0 \\ 0 & \frac{1}{V}\end{bmatrix}\begin{bmatrix}\frac{1}{\rho_V} & 0 \\ 0 & \frac{1}{\rho_\gamma}\end{bmatrix}\right\| \times \dots \\ & \dots \times \left\|\begin{bmatrix}-D - mg\sin\gamma - m\dot{V}_d - m\dot{\rho}_V\xi_V \\ LV - mg\cos\gamma - mV\dot{\gamma}_d - mV\dot{\rho}_\gamma\xi_\gamma\end{bmatrix}\right\|\end{aligned} \tag{22}$$

for a positive constant $\bar{k}$. Notice that the negative quadratic term in (22) dominates the second positive term, for large transformed errors ϵ_V, ϵ_γ; thus $\dot{\mathcal{L}}$ becomes negative, and consequently the value of the Lyapunov function $\mathcal{L}$ as well as of the errors ϵ_V, ϵ_γ remains bounded, ensuring according to Subsection II-A that the actual airspeed velocity and flight-path angle errors $e_V(t)$ and $e_\gamma(t)$ satisfy the performance specifications encapsulated in the corresponding performance functions, in view of $\|e_V(t)\| < \rho_V(t)$ and $\|e_\gamma(t)\| < \rho_\gamma(t)$, $\forall t \geq 0$. The rest of the stability analysis for the pitch angle θ and pitch rate q follows identical steps with [16], and is omitted here owing to page limitations.

C. Adaptive Identification

Consider the UAV-dynamics (2), (3) and (5), expressed as:

$$\begin{aligned}\dot{V} &= f_V(\alpha, V, \gamma) + g_V(\alpha, V)\Phi \\ \dot{\gamma} &= f_\gamma(\alpha, V, \gamma) + g_\gamma(\alpha, V)\Phi \\ \dot{q} &= f_q(\alpha, V, q) + g_q(\alpha, V, q)\delta\epsilon\end{aligned} \tag{23}$$

where the unknown functions $f_i(\cdot)$, $g_i(\cdot)$, $i \in \{V, \gamma, q\}$ will be substituted by RBF-NN approximants in the form of (7), plus a modeling error term as $f_i(\cdot) = Z_{f_i}^T(\cdot)W_{f_i} + \varepsilon_{f_i}(\cdot)$, $g_i(\cdot) = Z_{g_i}^T(\cdot)W_{g_i} + \varepsilon_{g_i}(\cdot)$, $i \in \{V, \gamma, q\}$, for some unknown weights W_{f_i}, W_{g_i} that minimize the modeling errors $\varepsilon_{f_i}(\cdot)$, $\varepsilon_{g_i}(\cdot)$ respectively, over a compact set. However, notice that (23) is not in the linear regression form (8), for which the DREM approach may be applied, since its left hand side is not measurable. To that end, we employ a standard filtering technique [17] to formulate a linear regression problem as follows:

$$\begin{aligned}y_V &\triangleq V - \frac{a}{s+a}V = \frac{1}{s+a}\left(Z_{f_V}^T W_{f_V} + \Phi Z_{g_V}^T W_{g_V}\right) \\ y_\gamma &\triangleq \gamma - \frac{a}{s+a}\gamma = \frac{1}{s+a}\left(Z_{f_\gamma}^T W_{f_\gamma} + \Phi Z_{g_\gamma}^T W_{g_\gamma}\right) \\ y_q &\triangleq q - \frac{a}{s+a}q = \frac{1}{s+a}\left(Z_{f_q}^T W_{f_q} + \delta_\epsilon Z_{g_q}^T W_{g_q}\right)\end{aligned} \tag{24}$$

where $a > 0$ denotes the pole of the adopted filter $\frac{1}{s+a}$. Consequently, we may apply the DREM technique presented in Subsection II-C for (24), and design decoupled adaptive laws in the form of (12), to estimate the unknown parameters.

Theorem 1: Consider the UAV longitudinal dynamics (1)-(5) as well as appropriately selected RBF-NNs with unknown synaptic weights to approximate the unknown nonlinearities in (23), within a compact domain of operation. If the airspeed velocity and altitude reference trajectories $V_d(t)$ and $h_d(t)$ are selected such that the adopted RBF-regressor vector is persistently exciting, then the control protocol presented in Subsection III-A and the DREM-based adaptive scheme presented in Subsection III-C, guarantee actual learning of the UAV longitudinal dynamics.

Remark 3: Note that for the adequate reference trajectories our algorithm guarantees the satisfaction of PE condition. This important attribute derives from the output tracking performance imposed by the PPC methodology. In particular, by choosing the performance parameters ρ_∞^V, ρ_∞^γ close to zero, then in each period there exists a minimum amount of time in which the airspeed velocity V as well as the altitude h of the vehicle lie within a neighborhood around each RBF center c_i, which implies the satisfaction PE condition. Furthermore, the model-free control strategy inherited by the PPC approach, reduces the interconnections between the trajectory tacking and system identifications problem, rendering our control scheme robust to system uncertainties, internal faults and external disturbances.

IV. Simulation Results

In this section, we present extensive simulation results that verify and clarify both the effectiveness of the proposed control protocol as well as the learning capabilities of the DREM-based identification scheme using RBF-NNs. For simulation purposes, the nonlinear dynamical model of the Aerosonde UAV was adopted, as presented in [14].

A. Control Design Efficiency

The proposed PPC scheme for the longitudinal UAV dynamics is employed to accurately track the following sinusoidal airspeed and altitude trajectory profiles $V_d(t) = 50 + 5\sin(2\pi 0.01t)$ and $h_d(t) = 100 + 80\sin(2\pi 0.01t)$. Given the initial conditions, the performance functions were selected as $\rho_V(t) = (50-5)e^{-0.5t} + 5$, $\rho_\gamma(t) = (\frac{\pi}{3} - \frac{\pi}{16})e^{-0.5t} + \frac{\pi}{16}$, $\rho_\theta(t) = (\pi - \frac{\pi}{20})e^{-0.5t} + \frac{\pi}{20}$, $\rho_q(t) = (\pi - \frac{\pi}{5})e^{-0.5t} + \frac{\pi}{5}$, with the control gains $k_h = 0.25, k_V = 2, k_\gamma = 10, k_\theta = 1, k_q = 0.35$ to produce reasonable control effort. In Fig.1a, the airspeed and altitude response is depicted, along with the desired profiles. The associated errors are illustrated in Fig.1b

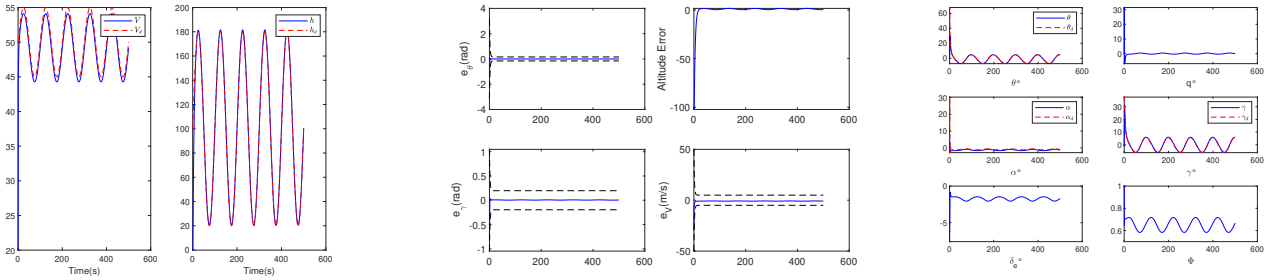

(a) The airspeed and altitude tracking. (b) The tracking errors. (c) System states and control signals.

Fig. 1: The closed loop system response for sinusoidal airspeed and altitude reference profiles.

along with the corresponding performance bounds encapsulated by the appropriately selected performance functions. Finally, the evolution of the rest of the system states, as well as the required control input signals are drawn in Fig.1c.

Robustness: To perform a more realistic simulation, wind disturbance in the form of Dryden gusts affecting the UAV dynamics and sensor models under white measurement noise, with zero mean and 10% deviation from the actual value, were considered. To that end, an Extended Kalman Filter (EKF) was adopted to provide the state estimates to the controller. The system's response is illustrated in Fig.2, from which the robustness of our method against external disturbances and measurement noise is verified.

Comparative Results: The proposed controller is compared to a classic model-based controller, designed, after linearizing the dynamics around the operating point, via the Successive Loop Closure with PD and PI controllers with appropriately selected gains such that the bandwidth of the outer(s) loop(s) is smaller by a factor of $10-15$ from the preceding loop(s) [14]. Notice in Fig.3a, that the aforementioned model-based controller achieves satisfactory tracking for slow varying airspeed and altitude profiles $V_d(t) = 50 + 5\sin(2\pi 0.01t)$ and $h_d(t) = 100 + 80\sin(2\pi 0.01t)$. However, when a more aggressive (faster) profile is adopted, i.e., $V_d(t) = 50 + 5\sin(2\pi 0.03t)$ and $h_d(t) = 300 + 200\sin(2\pi 0.03t)$, and without modifying the corresponding control gains, the model-based controller fails, as illustrated in Fig.3b. On the contrary, our control scheme preserves its satisfactory performance, without altering the control parameters, as depicted in Fig.3c. In particular, from Figs.3b,3c it can be observed that our method outperforms the model-based controller regarding to tracking delay, as well as to the amplitude of the the tracking error, which is more clear in the bottom subfigures of Figs.3b,3c, i.e., the tracking performance of altitude trajectory.

B. DREM-based Identification

It can be easily observed by (24) that the longitudinal UAV dynamics may be formulated as three, independent

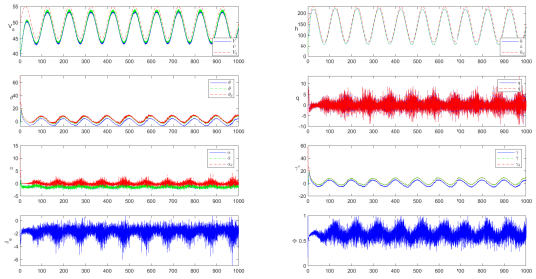

Fig. 2: The response under noise and disturbances.

linear regression problems. Hence, we employ three different RBF-NNs, one for each state variable of the UAV dynamics (i.e., V, q and γ), but with common regressor terms for the corresponding drift (f_V, f_q, f_γ) and input gain (g_V, g_q, g_γ) nonlinearities. The centers of each RBF-NN were selected through a k-means clustering algorithm, while the deviation was computed so that neighboring centers have a 75% overlap. Furthermore, since the proposed model-free controller guarantees predetermined transient and steady state performance, we selected via a trial and error procedure, appropriate airspeed and altitude reference trajectories such that the system state periodically visits the adopted RBF centers and hence ensures the satisfaction of the PE condition for the underlying RBF-NNs. Alternatively, we could choose reference signals consisting of $m \geq \frac{n}{2}$ ($n = 3$), discrete frequencies, which constitutes PE of order n. The parameter estimate errors are illustrated in Fig.4. Indicative results that verify the learning capabilities of the proposed scheme regarding the convergence of the parameter estimates related to the airspeed dynamics are presented in Table I. Finally, it should be noted that the identification procedure was conducted in the presence of noise affecting the sensor measurements.

Comment 1. The choice of the LTI filters in the DREM algorithm was critical in the identification scheme. Their parameters were selected after a tedious trial-and-error pro-

Manuscript 14 submitted to 2022 10th International Conference
on Systems and Control. Received August 13, 2022.

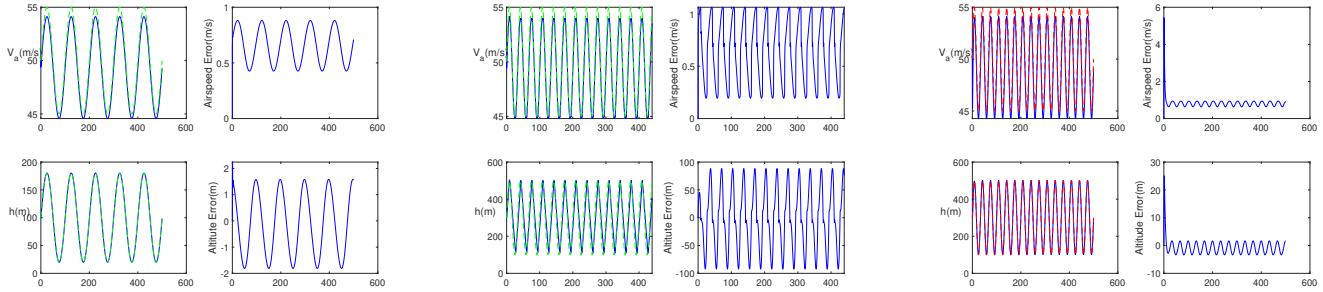

(a) Model-based controller (slow). (b) Model-based controller (fast). (c) The proposed controller (fast).

Fig. 3: Comparative simulation study. The airspeed and altitude response of a model-based and the proposed model-free controller for sinusoidal airspeed and altitude reference profiles.

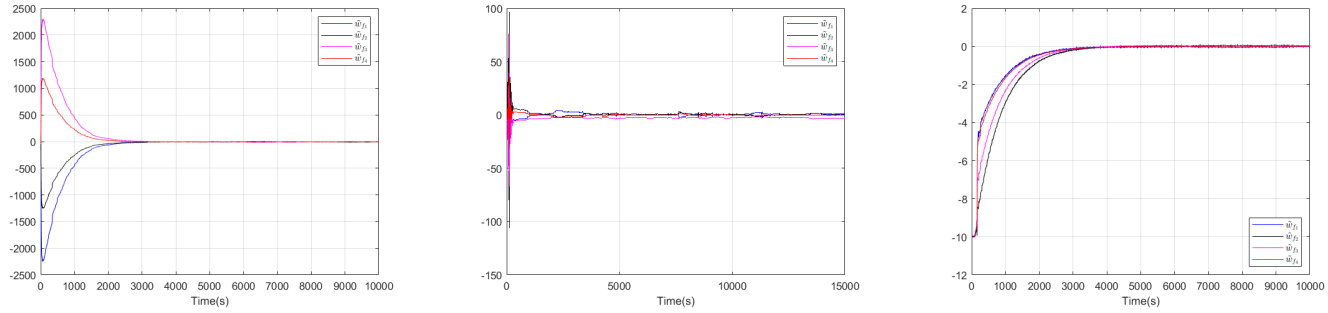

(a) Nonlinearity f_V. (b) Nonlinearity f_q. (c) Nonlinearity f_γ.

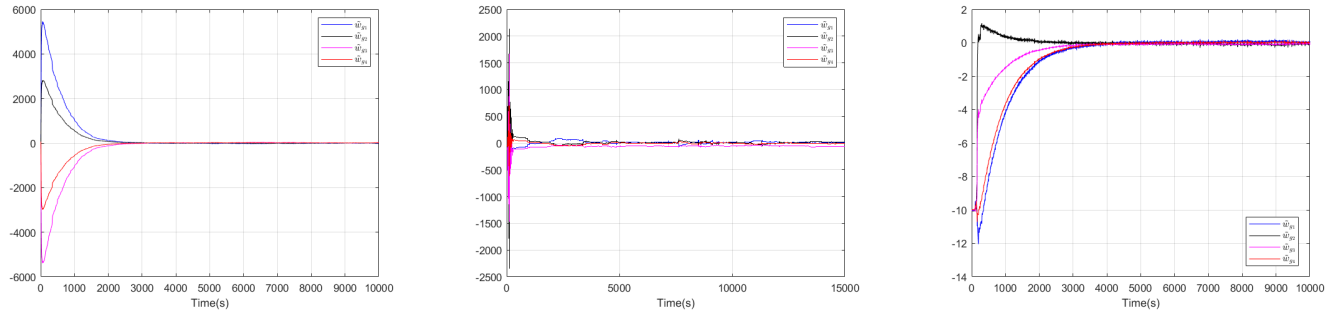

(d) Nonlinearity g_V. (e) Nonlinearity g_q. (f) Nonlinearity g_γ.

Fig. 4: The evolution of the parametric error for the RBF-NN weights.

cedure, since no indications exist on how to select them in a systematic way [18]. Nevertheless, an observation was that as the number of NN-weights grew, larger values for the filters' DC-gains α_i were needed to attain a sufficiently large value of $\det(M_e)$ to enable identification. As a result, it was necessary to select a rather small network with $q = 4$ nodes for each output, because a large DC-gain in the DREM operators would also magnify the modelling error of the RBF-NN, resulting in worse response. As for the filters' poles β_i, the only observation was that the higher the frequency of the trajectory was, the faster the poles should be selected to increase the value of $\det(M_e)$. Regarding the adaptation gains γ_i, increasing their values leads to faster rate of convergence in the expense of larger overshoot until the filters' state reach the steady state. Finally, it should be highlighted that the RBF-NN modelling error was probably

TABLE I: Results for the airspeed-related parameters. The optimal weights w_f^*, w_g^* were calculated via a batch-LS method.

w_f^*	$\hat{w}_f$	$\tilde{w}_f$ (%)	w_g^*	$\hat{w}_g$	$\tilde{w}_g$ (%)
-40.26	-36.51	9.31	60.75	56.7	-6.67
-45.35	-41.85	7.72	60.88	53.5	-12.12
-20.45	-22.53	-10.17	60.99	64.3	5.43
-16.26	-15.17	6.70	61.02	57.55	-5.69

the most critical factor in our identification scheme, since reducing it via adopting a more complex network structure, needs proper attention to avoid large filter DC-gains that deteriorate the achieved performance.

Comment 2. Systematic approaches on how to select the RBF-NN hidden layer parameters to enhance their approximation capabilities are well documented in the related literature and are not in the scope of this study. Nevertheless, concerning the RBF centers, we had to make sure that they were selected in a concise way, such that the UAV system states can actually attain their values during a reasonable flight. Therefore, sampled states from various maneuvers were given as inputs to the k-means algorithm that was employed to extract the RBF centers. Finally, it was observed that adding a bias term in the network output required larger DC-gains for the DREM operators, and thus was omitted.

V. Conclusions and Future Work

In this work, an adaptive learning scheme for small-scale fixed wing UAVs was developed, combining innovatively the DREM technique with the PPC methodology to establish provably correct identification of the UAV longitudinal dynamics. The proposed control scheme exhibits great robustness against model uncertainties and external disturbances, by decoupling the tracking controller from the system identification procedure. Future efforts will be devoted towards the experimental validation of the proposed scheme for sufficiently large flight envelope, involving take-off, landing and lateral motion profiles.

References

[1] J. Park and I. W. Sandberg, "Universal approximation using radial-basis-function networks," *Neural Computation*, vol. 3, no. 2, pp. 246–257, 1991.

[2] L. Ljung, *System Identification: Theory for the User*. USA: Prentice-Hall, Inc., 1986.

[3] S. Sastry and M. Bodson, *Adaptive Control: Stability, Convergence, and Robustness*. USA: Prentice-Hall, Inc., 1989.

[4] R. M. Sanner and J. E. Slotine, "Stable recursive identification using radial basis function networks," in *1992 American Control Conference*, pp. 1829–1833, 1992.

[5] A. Kurdila, F. J. Narcowich, and J. D. Ward, "Persistency of excitation in identification using radial basis function approximants," *SIAM journal on control and optimization*, vol. 33, no. 2, pp. 625–642, 1995.

[6] D. Gorinevsky, "On the persistency of excitation in radial basis function network identification of nonlinear systems," *IEEE Transactions on Neural Networks*, vol. 6, no. 5, pp. 1237–1244, 1995.

[7] Songwu Lu and T. Basar, "Robust nonlinear system identification using neural-network models," *IEEE Transactions on Neural Networks*, vol. 9, no. 3, pp. 407–429, 1998.

[8] S. Aranovskiy, A. Bobtsov, R. Ortega, and A. Pyrkin, "Performance enhancement of parameter estimators via dynamic regressor extension and mixing*," *IEEE Transactions on Automatic Control*, vol. 62, no. 7, pp. 3546–3550, 2017.

[9] S. Aranovskiy, A. Bobtsov, R. Ortega, and A. Pyrkin, "Improved transients in multiple frequencies estimation via dynamic regressor extension and mixing," *IFAC-PapersOnLine*, vol. 49, no. 13, pp. 99 – 104, 2016. 12th IFAC Workshop on Adaptation and Learning in Control and Signal Processing ALCOSP 2016.

[10] A. A. Bobtsov, A. A. Pyrkin, R. Ortega, S. N. Vukosavic, A. M. Stankovic, and E. V. Panteley, "A robust globally convergent position observer for the permanent magnet synchronous motor," *Automatica*, vol. 61, pp. 47 – 54, 2015.

[11] A. Bobtsov, D. Bazylev, A. Pyrkin, S. Aranovskiy, and R. Ortega, "A robust nonlinear position observer for synchronous motors with relaxed excitation conditions," *International Journal of Control*, vol. 90, no. 4, pp. 813–824, 2017.

[12] J. Choi, K. Nam, A. A. Bobtsov, A. Pyrkin, and R. Ortega, "Robust adaptive sensorless control for permanent-magnet synchronous motors," *IEEE Transactions on Power Electronics*, vol. 32, no. 5, pp. 3989–3997, 2017.

[13] C. P. Bechlioulis and G. A. Rovithakis, "Robust adaptive control of feedback linearizable mimo nonlinear systems with prescribed performance," *IEEE Transactions on Automatic Control*, vol. 53, no. 9, pp. 2090–2099, 2008.

[14] R. W. Beard and T. W. McLain, *Small Unmanned Aircraft: Theory and Practice*. USA: Princeton University Press, 2012.

[15] C. P. Bechlioulis and G. A. Rovithakis, "Prescribed performance adaptive control for multi-input multi-output affine in the control nonlinear systems," *IEEE Transactions on Automatic Control*, vol. 55, no. 5, pp. 1220–1226, 2010.

[16] C. P. Bechlioulis and G. A. Rovithakis, "A low-complexity global approximation-free control scheme with prescribed performance for unknown pure feedback systems," *Automatica*, vol. 50, no. 4, pp. 1217 – 1226, 2014.

[17] R. Middleton and G. Goodwin, "Adaptive computed torque control for rigid link manipulations," *Systems & Control Letters*, vol. 10, no. 1, pp. 9 – 16, 1988.

[18] D. N. Gerasimov, R. Ortega, and V. O. Nikiforov, "Relaxing the high-frequency gain sign assumption in direct model reference adaptive control," *European Journal of Control*, vol. 43, pp. 12 – 19, 2018.